Composites Science and Technology 69 (2009) 1841–1846

Contents lists available at ScienceDirect

Composites Science and Technology

journal homepage: www.elsevier.com/locate/compscitech

Piezoresistivity of unidirectional carbon/epoxy composites for multiaxial loading

Akira Todoroki [a,*], Yusuke Samejima [b], Yoshiyasu Hirano [c], Ryosuke Matsuzaki [a]

[a] Department of Mechanical Sciences and Engineering, Tokyo Institute of Technology, 2-12-1, O-okayama, Meguro, Tokyo 1528552, Japan
[b] Graduate Student of Tokyo Institute of Technology, 2-12-1, O-okayama, Meguro, 1528552, Tokyo, Japan
[c] Supersonic Transport Team, Aviation Program Group, Japan Aerospace Exploration Agency, 6-13-1 Osawa, Mitaka-shi, Tokyo 181-0015, Japan

ARTICLE INFO

Article history:
Received 3 February 2009
Received in revised form 24 March 2009
Accepted 25 March 2009
Available online 2 April 2009

Keywords:
A. Carbon fibres
A. Polymer–matrix composites
B. Electrical properties
A. Smart materials

ABSTRACT

The applied strain of carbon fibre reinforced plastics (CFRPs) is measurable by their electrical resistance changes. For damage monitoring of laminated CFRPs, piezoresistivity strongly affects the measured electrical resistance change through residual strain relief attributable to delamination cracks. Although several studies of CFRP laminates' piezoresistivity have been published, this study uses single-ply CFRP for specific piezoresistivity measurements in four directions. A review of the theory of in-plane piezoresistivity reveals orthotropic properties of CFRP piezoresistivity. In the present study, piezoresistivity of multiaxial loading is derived, and the unsymmetrical piezoresistivity matrix is calculated using the measured piezoresistivity here. Effects of multiaxial loading in a misaligned unidirectional laminate are also discussed here. The misaligned laminate causes large shrink in the transverse direction during tensile tests; poor electrical contacts at electrodes increases the electric current in the transverse direction; these two effects cause decrease of electrical resistance for the poor electrical contact specimen with large fibre misalignment.

1. Introduction

Carbon fibre reinforced polymer (CFRP) composites are widely adopted for aerospace and automobile components because of their high specific strength and stiffness. Interlaminar strength of the laminated composites, however, persists as a weak point for laminated CFRP structures. The great difficulty in finding internal delaminations by visual inspection persists as an important barrier to practical application of laminated composites.

The CFRP laminated structures are electrically conductive materials. For that reason, CFRP laminates can be used as self-sensing structures using electrical resistance changes [1–7]. Along with sensing of applied strain using electrical resistance changes, fibre breakage, fatigue damage, delamination, and matrix cracking have been detected. The authors' group has been examining electrical resistance change methods for monitoring locations and dimensions of damage such as delaminations and matrix cracks of laminated CFRPs [8–12]. Measurements of multiple point electrical resistance changes have enabled us to identify delamination locations and dimensions in laminated CFRP plates. Although delamination increases the electrical resistance, the measured electrical resistance decreased after delamination creation for thick laminated CFRPs [11]. In a thick CFRP beam, the delamination cracks originated in the middle of the beam because of the higher shear stress at the beam's middle. The electric current flowed only near the surface; the delamination cracks did not impede the electric current's path. Residual strain relief at the surface ply attributable to the delamination cracks is supposed to decrease the electrical resistance, which indicates that the piezoresistivity (electrical resistance change caused by applied strain) of CFRP may be significant, even for damage monitoring of laminated CFRPs.

In fact, several researchers have studied CFRP piezoresistivity [13–19]. Xiao et al. showed the thin plate theory of anisotropic piezoresistivity of laminated CFRP [13]. Ogi and Takao created an electrical resistance circuit model to measure anisotropic surface resistivity [15]. Wang and Chung experimentally discovered negative piezoresistivity of CFRP: the electrical resistance in the fibre direction decreases with the increased applied tensile strain in the fibre direction [14]. Angelidis et al. described the effect of electrical contact on negative piezoresistivity [16]. Negative piezoresistivity was investigated in detail by Wang and Chung [19]. All of these studies used laminated CFRP plates for experiments; the anisotropic piezoresistivity of a single-ply CFRP has not been described in detail. Moreover, piezoresistivity of multidirectional loading has not been discussed although the piezoresistivity of multidirectional loading is indispensable for analyses of the effect of residual stress relief in delamination monitoring of thick CFRP laminates.

In this report, the theory of thin anisotropic surface piezoresistivity of CFRPs is reviewed first. Using a single-ply CFRP, all anisotropic gage factors are measured experimentally. Using the single-ply is important to prevent the effect of ply misalignment and electric current in the thickness direction. The mechanisms

* Corresponding author. Tel./fax: +81 3 5734 3178.
E-mail address: atodorok@ginza.mes.titech.ac.jp (A. Todoroki).

0266-3538/$ - see front matter © 2009 Elsevier Ltd. All rights reserved.
doi:10.1016/j.compscitech.2009.03.023

of the anisotropic gage factors are also discussed. Based on measured gage factors, a formula to represent the electrical resistance changes in multiaxial loading is made here without using a simplified model. The formula enables us to estimate the negative piezoresistivity attributable to fibre misalignments. The mechanism of the negative piezoresistivity is discussed herein.

2. Review and discussion of theory of anisotropic piezoresistivity

For a thin CFRP ply, two-dimensional representation of piezoresistivity is applicable [13,15]. The surface electrical resistance R_i ($i = 1, 2$) of the CFRP ply is expressed as

$$R_i = \beta_i \frac{L_i}{W_i} \tag{1}$$

where $i = 1$ represents the fibre direction and $i = 2$ represents the transverse direction. In addition, β_i signifies the surface resistivity, L_i is the CFRP ply length and W_i is its width. Using Eq. (1), the fraction of electrical resistance change $\Delta R_i/R_i$ can be expressed as shown below.

$$\frac{\Delta R_i}{R_i} = \frac{\Delta \beta_i}{\beta_i} + \frac{\Delta L_i}{L_i} - \frac{\Delta W_i}{W_i} \tag{2}$$

For a 0°-ply specimen, a test of 0°-tension and 0°-electric current application (0–0) yields

$$\frac{\Delta R_{11}}{R_{11}} = \frac{\Delta \beta_1}{\beta_1} + (1 + \nu_{12})\varepsilon_1, \tag{3}$$

where the first subscript of R denotes the direction of electric current and the second subscripts represent the loading direction.

For a 0°-ply specimen, a test of 0°-tension and 90°-electric current application (0–90) is

$$\frac{\Delta R_{21}}{R_{21}} = \frac{\Delta \beta_2}{\beta_2} - (1 + \nu_{12})\varepsilon_1 = \frac{\Delta \beta_2}{\beta_2} + \left(1 + \frac{1}{\nu_{12}}\right)\varepsilon_2 \tag{4}$$

For a 90°-ply specimen, a test of 90°-tension and 90°-electric current application (90–90) suggests the following equation:

$$\frac{\Delta R_{22}}{R_{22}} = \frac{\Delta \beta_2}{\beta_2} + (1 + \nu_{21})\varepsilon_2 \tag{5}$$

For a 90°-ply specimen, a test of 90°-tension and 0°-electric current application (90–0) gives the following equation:

$$\frac{\Delta R_{12}}{R_{12}} = \frac{\Delta \beta_1}{\beta_1} - (1 + \nu_{21})\varepsilon_2 = \frac{\Delta \beta_1}{\beta_1} + \left(1 + \frac{1}{\nu_{21}}\right)\varepsilon_1 \tag{6}$$

The constitutive relation between the increments of piezoresistivity $\Delta\beta_i$ and normal strain of two-dimensional representations can be expressed as

$$\begin{bmatrix} \Delta\beta_1 \\ \Delta\beta_2 \end{bmatrix} = \begin{bmatrix} C_{11} & C_{12} \\ C_{21} & C_{22} \end{bmatrix} \begin{bmatrix} \varepsilon_1 \\ \varepsilon_2 \end{bmatrix} \tag{7}$$

where C_{ij} denotes the surface piezoresistivity tensor.

After substitution of Eq. (7) into Eqs. (3)–(6), the piezoresistivity gage factor k_{ij} is obtained as follows:

$$k_{11} = \frac{\Delta R_{11}/R_{11}}{\varepsilon_1} = \frac{C_{11} - \nu_{12}C_{12}}{\beta_1} + (1 + \nu_{12}) \tag{8}$$

$$k_{12} = \frac{\Delta R_{12}/R_{12}}{\varepsilon_1} = \frac{C_{11} - C_{12}/\nu_{21}}{\beta_1} + \left(1 + \frac{1}{\nu_{21}}\right) \tag{9}$$

$$k_{21} = \frac{\Delta R_{21}/R_{21}}{\varepsilon_2} = \frac{C_{22} - C_{21}/\nu_{12}}{\beta_2} + \left(1 + \frac{1}{\nu_{12}}\right) \tag{10}$$

$$k_{22} = \frac{\Delta R_{22}/R_{22}}{\varepsilon_2} = \frac{C_{22} - \nu_{21}C_{21}}{\beta_2} + (1 + \nu_{21}) \tag{11}$$

In those equations, the first subscript of k_{ij} denotes the direction of electric current The second subscript signifies the direction of loading. Eqs. (8) and (9) show that k_{11} is not equal to k_{12}. Eqs. (10) and (11) show similarly that k_{21} is not equal to k_{22}.

Although earlier reports [13–15] do not specifically describe them, these differences are important because the measured fraction of electrical resistance change is not directly proportional to the measured uniaxial strain. For example, the difference between k_{11} and k_{12} means that the fraction of electrical resistance change in the fibre direction must be counted separately into the two: strain caused by loading in the fibre direction and the strain caused by loading in the transverse direction. For the analyses of electrical resistance changes of delaminated CFRP, the piezoresistivity of multiaxial loading is indispensable.

3. Experimental methods and results

3.1. Materials and specimens

The material used here for experiments is a carbon/epoxy prepreg (PYROFIL #380; Mitsubishi Rayon Co. Ltd.). The fibres used are TR30S 12 l (tensile strength 4410 MPa, tensile modulus 235 GPa); the epoxy resin is a product designed for general use. Curing conditions are 130 °C × 90 min under vacuum pressure.

For measurements of electrical resistance changes, small single-ply specimens of 30 mm × 30 mm × 0.23 mm (thickness) are adopted here. The fibre volume fraction of these specimens is approximately 60%. The small specimens are adopted here to prevent a change in electrical resistance at an undesired electric current path in a large specimen, such as a clamped area. The specimens are too small. Therefore, the specimens are attached on the surface of a base specimen made from an eight-0°-ply laminate or an eight-90°-ply laminate. The base specimen is 200 mm long, with 30 mm wide and 2 mm thick. Configurations of the base specimens and target specimens are presented in Fig. 1.

In the target specimen, electrical copper plating method is applied to make electrical contact to carbon fibres after polishing the specimen surface to remove the surface resin. Four electrodes are prepared in a specimen to use the four-probe method to measure electrical resistance change. The spacing between the electrodes is presented in Fig. 1.

Base specimens of two types were prepared: a base specimen of stacking sequence of $[0_8]_T$ was created from the same prepreg for the tensile test to the fibre direction. A base specimen of the stacking sequence of $[90_8]_T$ was made from the same prepreg used for the tensile test of the transverse direction. On the $[0_8]_T$ base specimen, two target specimens are attached as presented in Fig. 1. Both target specimens are loaded in the fibre direction but the electric current directions differ. The same size target specimens are attached on the other side surface at the same positions to prevent generation of a bending moment. The electric current must flow only in the target specimens. For that reason, the base specimen surface is coated with epoxy resin as an insulator before attaching the target specimens. Perfect insulation between the target specimen and the base specimen was confirmed using a commercially available LCR meter (type #3520; Hioki Co. Ltd.).

Lead wires are soldered to the electrodes of the target specimens. To measure the electrical resistance change of the target specimen, the four-probe method is adopted here. An LCR meter (Hioki Co. Ltd.) is used with 1.5 kHz alternating current of 10 mA. The alternating current is used here because the LCR meter provided smaller variation and the CFRP can be regarded as a simple resistance for this lower frequency.

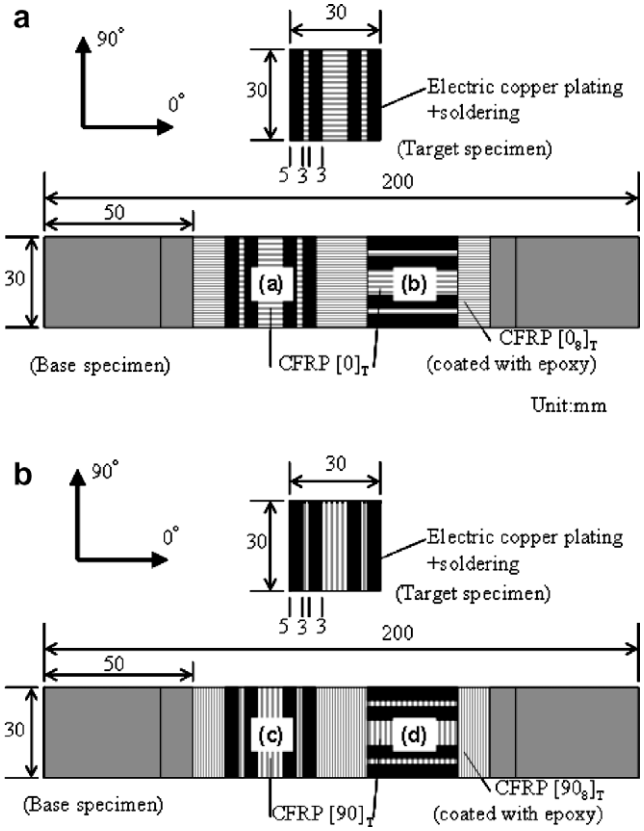

Fig. 1. Specimen configuration. (a) Unidirectional fibre-direction loading and (b) unidirectional transverse-direction loading.

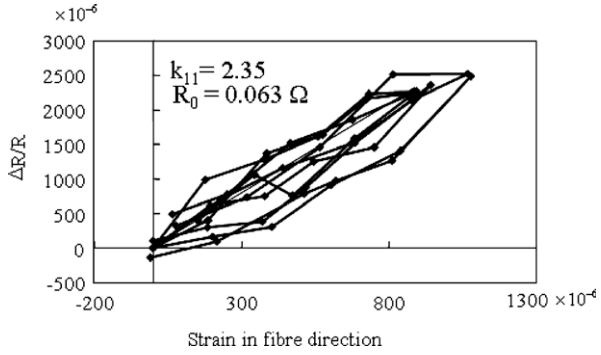

Fig. 2. Measured electrical resistance change in fibre-direction loading of fibre-direction current path.

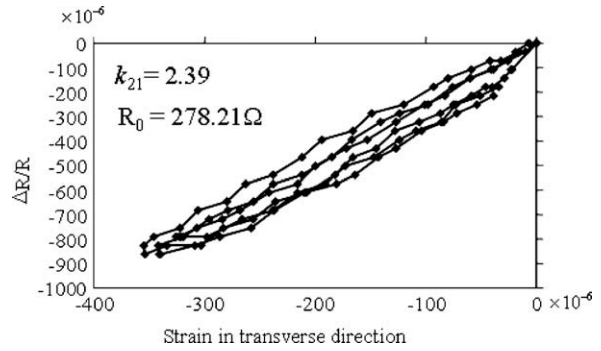

Fig. 3. Measured electrical resistance change in fibre-direction loading of transverse-direction current path.

Using the base specimen of $[0_8]_T$, tensile tests of two types are performed here. In one target specimen, the electric current flows in the fibre direction. This type is called a 0–0 specimen herein: the first figure 0 represents the tensile direction and the second figure 0 signifies the electric current direction. In the other target specimen, electric current flows in the transverse direction. This type is called a 0–90 specimen herein. Similarly, tensile tests of two types are performed here using the base specimen of $[90_8]_T$. The two types are 90–90 type and 90–0 type: the electric current flows in the transverse direction in the 90–90 type specimen and the electric current flows in the fibre direction in the 90–0 type specimen.

A bi-axial strain gage is attached in the middle of each target specimen to measure the applied strain of the target specimen. Glass fibre reinforced plastic tabs are attached on both ends to protect the base specimen. Tensile tests of loading speed of 0.5 mm/min are performed using a material testing machine (Shimadzu Corp.). All electrical resistance changes are measured in the elastic deformation region. Cyclic tests are conducted to measure the electrical resistance hysteresis in this study.

3.2. Results and discussion

Measured results of the 0–0-type test are presented in Fig. 2. In this test, the loading direction is the fibre direction and electric current flows in the fibre direction. The abscissa is the measured applied strain in the fibre direction, and the ordinate is the measured fraction of electrical resistance change. Several loading–unloading tests were performed for this study. Although the variance is larger than that of the conventional strain gage, the relation between the measured applied strain and the measured fraction of the electrical resistance change increases almost linearly with increased applied tensile strain. The gage factor is $k_{11} = 2.35$, which closely resembles the normal strain gage. This positive gage factor results from normal piezoresistivity of the carbon fibre itself.

Measured results of the 0–90-type test are depicted in Fig. 3. The abscissa is the measured strain attributable to Poisson's ratio; the ordinate is the measured fraction of the electrical resistance. The tensile strain is applied in the fibre direction. Therefore, the transverse strain is the compression strain. With increased the applied tensile strain (with the decrease of transverse compressive strain), the electrical resistance decreases. The gage factor k_{21} is 2.39 here. The results differ completely from published results [15–17]. Those previous papers all report that the transverse electrical resistance increases with the increase of applied tensile strain in the fibre direction. In previous papers, the transverse resistance increase can be explained using the fibre-contact-separation model as portrayed in Fig. 4. Fibre contacts are caused by the undulation of carbon fibres. Tensile loading in the fibre direction straightens the undulated fibres. Consequently, the tensile strain in the fibre direction decreases the fibre contact. In other words, the increase of electrical resistance in the transverse direction results from tensile loading in the fibre direction. This effect of fibre-contact-separation model should be discussed in detail in future research.

The results presented in Fig. 3 decrease with increased tensile loading in the fibre direction. The tensile strain in the fibre direction causes compression strain in the transverse direction. The compression strain decrease the fibres' spacing and increases the cross sectional area for the electric current in the transverse direction. This causes a decrease of electrical resistance in the transverse direction. As described in earlier papers, undulation of the fibres increases the electrical resistance in the transverse direction. These two effects are mutually competitive. The electrical

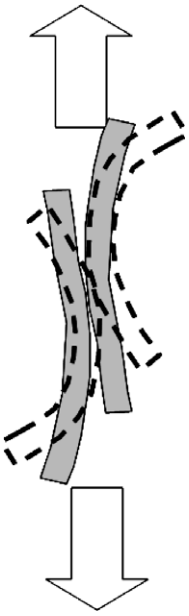

Fig. 4. Fibre-contact separation model to explain positive piezoresistivity in the transverse direction.

resistance in the transverse direction increases with increased tensile loading in the fibre direction when the effect of undulation of fibres is greater than the effect of compression. In Fig. 3, the effect of fibre undulation is apparently lower than the effect of compression in the transverse direction. This result shows that the piezoresistivity gage factor k_{21} might change markedly because of fibre undulation.

Measured results of the 90–90-type test are presented in Fig. 5. In this test, the loading direction is the transverse direction and electric current flows in the transverse direction. The abscissa shows the measured applied strain in the transverse direction; the ordinate shows the measured fraction of electrical resistance change. The relation between the measured applied stain and the measured fraction of the electrical resistance change is increasing linearly with the increase of applied tensile strain. The gage factor is k_{22} = 3.88; the value is larger than that of the normal strain gage. The higher gage factor results from the high sensitivity against the applied strain in the transverse direction: the contacts between adjacent fibres realize the electrical conductivity in the transverse direction, and the contact resistances have high sensitivity against the applied strain. This gage factor might also change because of the fibre undulation.

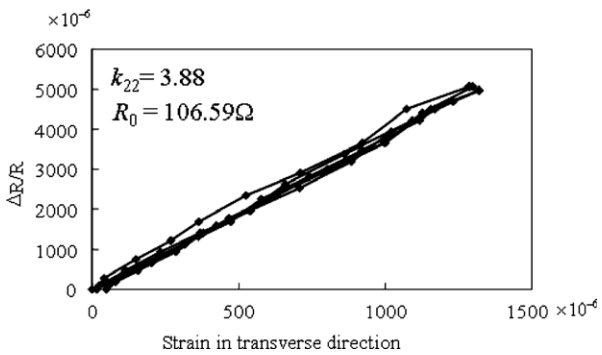

Fig. 5. Measured electrical resistance change in transverse-direction loading of transverse-direction current path.

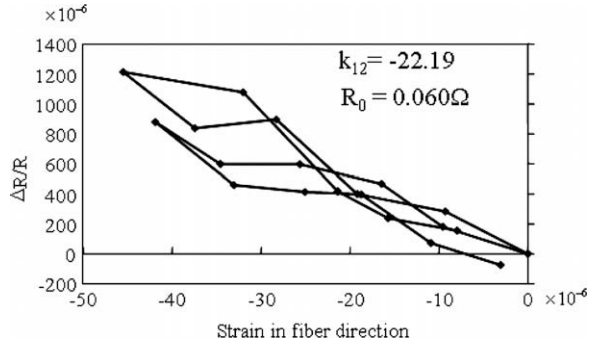

Fig. 6. Measured electrical resistance change in transverse-direction loading of fibre-direction current path.

Measured results of 90–0-type test are depicted in Fig. 6. In the test, the loading direction is the transverse direction and electric current flows in the fibre direction. The abscissa is the measured applied strain in the fibre direction caused by Poisson's ratio effect; the ordinate is the measured fraction of the electrical resistance change. The relation between the measured applied stain and the measured fraction of the electrical resistance change increases almost linearly with the increase of the applied tensile load and decrease of the measured transverse strain. The gage factor is $k_{12} = -22.19$. Although the strain in the fibre direction is compressive, the electrical resistance in the fibre direction increases. Therefore, the gage factors of k_{11} and k_{12} are completely different, although both are electrical resistance changes attributable to the strain of the fibre direction.

Negative piezoresistivity k_{12} means that electrical resistance in the fibre direction is affected by the electric current in the transverse direction. Fig. 7 exhibits this mechanism. Not all carbon fibres are perfectly straight in a ply. Fig. 7 portrays that fibre number 1 has a contact to the electrode A, but that fibre number 1 has no contact to the electrode B because of the fibre undulation. Therefore, the electric current must flow in the transverse direction to carbon fibre number 2, which contacts electrode B. Since there are a lot of fibres in the actual CFRP, there are a lot of fibres that have electrical contact to the electrodes even for the poor electrical contact specimen. The electrical resistance in the fibre direction is a combined effect of electrical current of the fibre direction and of the transverse direction.

The piezoresistivity k_{12} might be different when a couple of electrodes are mounted on both edges of the CFRP specimen, as shown for electrodes C and D in Fig. 7. Electric current in carbon fibres numbers 1 and 2 need not flow in the transverse direction when the electrodes are mounted on C and D. However, fibres are not always perfectly continuous along the specimen; moreover, all fibres have contact points between adjacent fibres at different distances from electrodes C and D: different distances from the electrodes mean that the contact points might have different

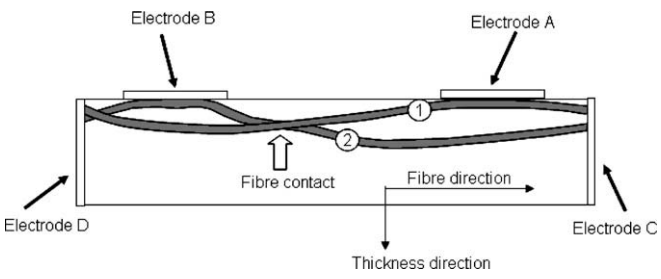

Fig. 7. Actual fibre undulation in a ply and effect of location of electrodes.

voltages. These mean that electric current might flow transversely even when the electrodes are mounted at both ends of the specimen. Therefore, the electrode locations affect the piezoresistivity, but the electrodes at the CFRP specimen edges are not free from piezoresistivity of the transverse direction.

4. Multiaxial loading

4.1. Piezoresistivity for multiaxial loading

As the experimental results show, the piezoresistivity of k_{11} differs from that of k_{12} and that of k_{22} differs from that of k_{21}. Consequently, the electrical resistance changes attributable to applied multiple loads are not directly proportional to the measured strain: the measured strain includes strain caused by lateral loading. To obtain the relation between the electrical resistance changes and the measured strains for the multiaxial loading, a new formula must be derived.

The measured strains ε_x and ε_y comprise strains derived from the applied load and strains derived from Poisson's ratio. First, these must be separated using the stress–strain relation. In the fibre direction (L) and transverse (T) coordinate, the stress–strain relation is written as follows:

$$\begin{Bmatrix}\sigma_L\\ \sigma_T\\ \tau_{LT}\end{Bmatrix}=\begin{bmatrix}Q_{11} & Q_{12} & 0\\ Q_{21} & Q_{22} & 0\\ 0 & 0 & Q_{66}\end{bmatrix}\begin{Bmatrix}\varepsilon_L\\ \varepsilon_T\\ \gamma_{LT}\end{Bmatrix} \tag{12}$$

$$Q_{11}=\frac{E_L}{1-\nu_{LT}\nu_{TL}},\quad Q_{12}=Q_{21}=\frac{\nu_{TL}E_L}{1-\nu_{LT}\nu_{TL}},$$
$$Q_{22}=\frac{E_T}{1-\nu_{LT}\nu_{TL}},\quad Q_{66}=G_{LT} \tag{13}$$

Let the x-axis be equal to the L-axis and the y-axis be equal to the T-axis. According to Eq. (12), the measured strains ε_x (ε_L) and ε_y (ε_T) are transformed into stresses σ_x (σ_L) and σ_y (σ_T). The obtained stresses σ_x (σ_L) and σ_y (σ_T) enable us to calculate the strain caused by the applied load (ε^A) and strain because of Poisson's ratio (ε^P). Using the compliance matrix, the stress–strain relation is expressed as shown below.

$$\begin{Bmatrix}\varepsilon_L\\ \varepsilon_T\\ \gamma_{LT}\end{Bmatrix}=\begin{bmatrix}S_{11} & S_{12} & 0\\ S_{21} & S_{22} & 0\\ 0 & 0 & S_{66}\end{bmatrix}\begin{Bmatrix}\sigma_L\\ \sigma_T\\ \tau_{LT}\end{Bmatrix} \tag{14}$$

$$S_{11}=\frac{1}{E_L},\quad S_{12}=S_{21}=-\frac{\nu_{TL}}{E_T},\quad S_{22}=\frac{1}{E_T},\quad S_{66}=\frac{1}{G_{LT}} \tag{15}$$

In this equation, the strain caused by the applied load and the strain attributable to Poisson's ratio are separable as the following:

$$\begin{aligned}\begin{Bmatrix}\varepsilon_L\\ \varepsilon_T\\ \gamma_{LT}\end{Bmatrix}&=\begin{Bmatrix}\varepsilon_L^A\\ \varepsilon_T^P\\ 0\end{Bmatrix}+\begin{Bmatrix}\varepsilon_L^P\\ \varepsilon_T^A\\ 0\end{Bmatrix}+\begin{Bmatrix}0\\ 0\\ S_{66}\tau_{LT}\end{Bmatrix}\\ &=\begin{Bmatrix}S_{11}\sigma_L\\ S_{21}\sigma_L\\ 0\end{Bmatrix}+\begin{Bmatrix}S_{12}\sigma_T\\ S_{22}\sigma_T\\ 0\end{Bmatrix}+\begin{Bmatrix}0\\ 0\\ S_{66}\tau_{LT}\end{Bmatrix}\\ &=\begin{bmatrix}S_{11} & S_{12} & 0\\ S_{21} & S_{22} & 0\\ 0 & 0 & S_{66}\end{bmatrix}\begin{Bmatrix}\sigma_L\\ \sigma_T\\ \tau_{LT}\end{Bmatrix}\end{aligned} \tag{16}$$

Using Eqs. (12) and (16), each strain can be derived as follows:

$$\begin{Bmatrix}\varepsilon_L^A\\ \varepsilon_L^P\\ \varepsilon_T^A\\ \varepsilon_T^P\end{Bmatrix}=\begin{bmatrix}S_{11}Q_{11} & S_{11}Q_{12}\\ S_{12}Q_{21} & S_{12}Q_{22}\\ S_{22}Q_{21} & S_{22}Q_{22}\\ S_{12}Q_{11} & S_{12}Q_{12}\end{bmatrix}\begin{Bmatrix}\varepsilon_L\\ \varepsilon_T\end{Bmatrix} \tag{17}$$

From the definition of piezoresistivity, the fraction of electrical resistance change $\Delta R/R$ of each direction can be derived as shown below.

$$\begin{aligned}\begin{Bmatrix}\left(\frac{\Delta R}{R}\right)_L\\ \left(\frac{\Delta R}{R}\right)_T\end{Bmatrix}&=\begin{bmatrix}k_{11} & k_{12} & 0 & 0\\ 0 & 0 & k_{21} & k_{22}\end{bmatrix}\begin{Bmatrix}\varepsilon_L^A\\ \varepsilon_L^P\\ \varepsilon_T^A\\ \varepsilon_T^P\end{Bmatrix}\\ &=\begin{bmatrix}k_{11} & k_{12} & 0 & 0\\ 0 & 0 & k_{21} & k_{22}\end{bmatrix}\begin{bmatrix}S_{11}Q_{11} & S_{11}Q_{12}\\ S_{12}Q_{21} & S_{12}Q_{22}\\ S_{22}Q_{21} & S_{22}Q_{22}\\ S_{12}Q_{11} & S_{12}Q_{12}\end{bmatrix}\begin{Bmatrix}\varepsilon_L\\ \varepsilon_T\end{Bmatrix}\\ &=\begin{bmatrix}k_{11}S_{11}Q_{11}+k_{12}S_{12}Q_{21} & k_{11}S_{11}Q_{12}+k_{12}S_{12}Q_{22}\\ k_{21}S_{22}Q_{21}+k_{22}S_{12}Q_{11} & k_{21}S_{22}Q_{22}+k_{22}S_{12}Q_{12}\end{bmatrix}\begin{Bmatrix}\varepsilon_L\\ \varepsilon_T\end{Bmatrix}\\ &=\mathbf{K}\begin{Bmatrix}\varepsilon_L\\ \varepsilon_T\end{Bmatrix}\end{aligned} \tag{18}$$

The multiaxial piezoresistivity matrix **K** is not symmetric; **K** depends on the elastic modulus. Substituting the elastic modulus of E_L = 141 GPa, E_T = 10 GPa, and ν_{LT} = 0.28 together with the measured piezoresistivity k_{ij} of Figs. 2, 3, 5 and 6, the piezoresistivity matrix **K** is calculable as presented below.

$$\begin{Bmatrix}\left(\frac{\Delta R}{R}\right)_L\\ \left(\frac{\Delta R}{R}\right)_T\end{Bmatrix}=\begin{bmatrix}2.49 & 0.43\\ -0.42 & 2.38\end{bmatrix}\begin{Bmatrix}\varepsilon_L\\ \varepsilon_T\end{Bmatrix} \tag{19}$$

Although the difference between k_{12} and k_{21} is small in the present composites, the piezoresistivity depends on the fibre undulation, as described in Section 3, which means that the multiaxial piezoresistivity depends on the fabrication process. The theory of piezoresistivity can be easily expanded to the 3-dimensional theory. That requires, however, to measure piezoresistivity in the thickness direction, and this is quite difficult for a single ply.

Usually, laminated composites include thermal residual strain. Delamination engenders residual strain relief. This residual strain relief is multiaxial strain relief. Eq. (19) is useful to estimate the effect of the residual strain relief on the measured electrical resistance change for delamination monitoring.

4.2. Effect of fibre misalignment

An actual laminated composite plate is not free from the fibre misalignment of each ply and fibre undulation in each ply. Even for unidirectional laminates such as $[0_4]_T$ as presented in Fig. 8, each ply has fibre misalignment of $[\theta_1/\theta_2/\theta_3/\theta_4]_T$. We consider that each electrode has poor electrical contact, as presented in Fig. 8.

We consider the case of a misaligned laminate of $[5/10/3/\text{-}10]_T$ with comparison of a perfect unidirectional laminate of $[0_4]_T$. The in-plane stiffness matrix **A** of each laminate and compliance matrix **a** are calculated as shown below.

For the misaligned laminate of $[5/10/3/-10]_T$, the following are true:

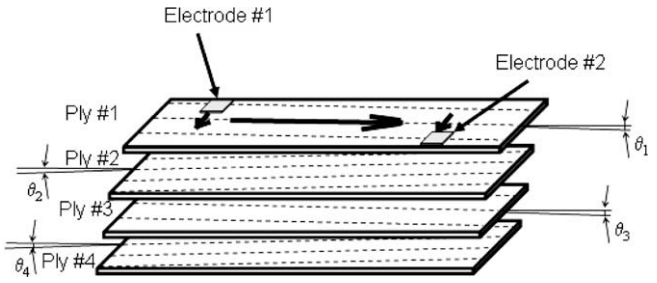

Fig. 8. Misaligned ply model of the unidirectional laminate and electric current path.

$$\mathbf{A}=\begin{bmatrix}A_{11}^m & A_{12}^m & A_{16}^m\\ A_{21}^m & A_{22}^m & A_{26}^m\\ A_{61}^m & A_{62}^m & A_{66}^m\end{bmatrix}=\begin{bmatrix}68.6\times10^6 & 2.5\times10^6 & 2.2\times10^6\\ 2.5\times10^6 & 5.1\times10^6 & 0.06\times10^6\\ 2.2\times10^6 & 0.06\times10^6 & 3.58\times10^6\end{bmatrix}(N/m)$$
$$\mathbf{a}=\begin{bmatrix}a_{11}^m & a_{12}^m & a_{16}^m\\ a_{21}^m & a_{22}^m & a_{26}^m\\ a_{61}^m & a_{62}^m & a_{66}^m\end{bmatrix}=\begin{bmatrix}1.79\times10^{-8} & -6.87\times10^{-9} & -1.41\times10^{-8}\\ -6.87\times10^{-9} & 1.99\times10^{-7} & -7.71\times10^{-10}\\ -1.41\times10^{-8} & -7.71\times10^{-10} & 3.40\times10^{-7}\end{bmatrix} \quad (20)$$

For the perfect unidirectional laminate of $[0_4]_T$, the following hold:

$$\mathbf{A}=\begin{bmatrix}A_{11}^0 & A_{12}^0 & A_{16}^0\\ A_{21}^0 & A_{22}^0 & A_{26}^0\\ A_{61}^0 & A_{62}^0 & A_{66}^0\end{bmatrix}=\begin{bmatrix}70.8\times10^6 & 1.4\times10^6 & 0\\ 1.4\times10^6 & 5.0\times10^6 & 0\\ 0 & 0 & 2.5\times10^6\end{bmatrix}(N/m)$$
$$\mathbf{a}=\begin{bmatrix}a_{11}^0 & a_{12}^0 & a_{16}^0\\ a_{21}^0 & a_{22}^0 & a_{26}^0\\ a_{61}^0 & a_{62}^0 & a_{66}^0\end{bmatrix}=\begin{bmatrix}1.42\times10^{-8} & -3.97\times10^{-9} & 0\\ -3.97\times10^{-9} & 2.0\times10^{-7} & 0\\ 0 & 0 & 4.0\times10^{-7}\end{bmatrix} \quad (21)$$

Therein, the ply thickness is set to 0.125 mm, and G_{LT} is 5.0 GPa. Consequently, each laminate's thickness is $h = 0.5\times10^{-3}$ m.

The measured tensile modulus E_L' is calculable using $E_L' = 1/(ha_{11})$. The difference between the modulus of the misaligned laminate and the modulus of the perfect unidirectional laminate is calculated as follows:

$$\frac{E_L^m}{E_L^0}=\frac{ha_{11}^0}{ha_{11}^m}=\frac{1.42}{1.79}=0.79 \quad (22)$$

On the other hand, the measured Poisson's ratio v_{LT}' is calculable using $v_{LT}' = -a_{21}/a_{11}$. The difference between the Poisson's ratio of the misaligned laminate and the Poisson's ratio of the perfect unidirectional laminate is calculated as

$$\frac{v_L^m}{v_L^0}=\frac{ha_{21}^m ha_{11}^0}{ha_{11}^m ha_{21}^0}=\frac{6.87\times1.42}{1.79\times3.97}=1.37 \quad (23)$$

The results of Eqs. (22) and (23) reveal that the fibre misalignment has a great effect on the transverse direction. For a tensile test of a fibre misaligned unidirectional laminate, the laminate is equal to the specimen subjected to multiaxial loading: the tensile load of the fibre direction and the compression load of the transverse direction.

For the actual unidirectional laminate, the electrodes have imperfect electrical contact and have poor sparse contact, as presented in Fig. 8, which shows that the electrical current of the fibre direction includes electric current in the transverse direction. Although the electrical path of the transverse direction is short, the current in the transverse direction has a large effect because the electrical resistivity in the transverse direction is more than 1000 times that of the fibre direction.

For the misaligned laminate, the laminate is subjected to the transverse compression load as described previously. Eq. (19) shows that the larger transverse compression strain might cause a large decrease of electrical resistance in the fibre direction and decrease the electrical resistance in the transverse direction too for the fibre misaligned laminate with sparse poor electrodes, which might be the negative piezoresistivity of the fibre direction of unidirectional CFRP in the reference [17].

Better electrical contact at electrodes decreases the electric current path in the transverse direction. That deletes the effect of electrical resistance decrease of the transverse direction. Consequently, negative piezoresistivity might improve to a positive one after polishing the surface, as described in an earlier report [17]. The perfect contact, however, not can delete the effect perfectly because there are a lot of fibres that have contact between fibres. The four-probe method is not entirely error-free because of the electrical contact at the electrodes for the strongly orthotropic CFRP.

5. Conclusions

This paper described examination of anisotropic piezoresistivity of unidirectional single-ply CFRP. Experiments were conducted using a small rectangular single-ply CFRP attached to the unidirectional CFRP laminate. Electrical resistance changes during loading of four patterns were measured experimentally. The in-plane piezoresistivity is reviewed theoretically herein and multidirectional loading relations between the electrical resistance changes and measured strains are derived here. The obtained results are as described below:

(1) Piezoresistivity of CFRP of multidirectional loading is obtained theoretically and experimentally.
(2) The multidirectional piezoresistivity matrix is not symmetric for CFRP.
(3) The electrical resistance change in the fibre direction is not directly proportional to the measured unidirectional strain of the carbon fibre, but it is affected by electric current in transverse direction.
(4) Fibre misalignment and sparse electrical contact at electrodes cause negative piezoresistivity.

References

[1] Schulte K, Baron Ch. Load and failure analyses of CFRP laminates by means of electrical resistivity measurements. Compos Sci Technol 1989;36(1):63–76.
[2] Muto N, Yanagida H, Nakatsuji T, Sugita M, Ohtsuka Y. Preventing fatal fractures in carbon-fibre–glass-fibre-reinforced plastic composites by monitoring change in electrical resistance. J Am Ceram Soc 1993;76(4):875–9.
[3] Wang X, Chung DDL. Continuous carbon fibre epoxy–matrix composite as a sensor of its own strain. Smart Mater Struct 1996;5(6):796–800.
[4] Irving PE, Thiagarajan C. Fatigue damage characterization in carbon fibre composite materials using an electrical potential technique. Smart Mater Struct 1998;7(4):456–66.
[5] Seo DC, Lee JJ. Damage detection of CFRP laminates using electrical resistance measurement and a neural network. Compos Struct 1999;47:525–30.
[6] Abry JC, Choi YK, Chateauminois A, Dalloz B, Giraud G, Salvia M. In-situ monitoring of damage in CFRP laminates by using AC and DC measurements. Compos Sci Technol 2001;61(6):855–64.
[7] Park JB, Okabe T, Takeda N, Curtin WA. Electromechanical modeling of unidirectional CFRP composites under tensile loading condition. Compos Part A 2002;33(2):267–75.
[8] Todoroki A. Effect of the number of electrodes as a diagnostic tool for delamination monitoring of graphite/epoxy laminates using electric resistance change. Compos Sci Technol 2001;61(13):1871–80.
[9] Todoroki A, Tanaka M, Shimamura Y. Measurement of orthotropic electric conductance of CFRP laminates and analysis of the effect on delamination monitoring with electric resistance change method. Compos Sci Technol 2002;62(5):619–28.
[10] Todoroki A, Tanaka M, Shimamura Y. High performance estimations of delamination of graphite/epoxy laminates with electric resistance change method. Compos Sci Technol 2003;63(13):1911–20.
[11] Todoroki A, Ueda M, Shimamura Y. Damage monitoring of a thick CFRP beam using electrical impedance changes. Key Eng Mater 2007;353–358:1298–301.
[12] Todoroki A, Omagari K. Detection of matrix crack density of CFRP using electrical potential change method with multiple probes. J Solid Mech Mater Eng JSME 2008;2(6):718–29.
[13] Xiao J, Li Y, Fan WX. A laminate theory of piezoresistance for composite laminates. Compos Sci Technol 1999;59(9):1369–73.
[14] Wang S, Chung DDL. Piezoresistivity in continuous carbon fibre polymer–matrix composite. Polym Compos 2000;21(1):13–9.
[15] Ogi K, Takao Y. Characterization of piezoresistance behaviour in a CFRP unidirectional laminate. Compos Sci Technol 2005;65(2):231–9.
[16] Angelidis N, Wei CZY, Irving PE. The electrical resistance response of continuous carbon fibre composite laminates to mechanical strain. Compos Part A 2004;35(10):1135–47.
[17] Todoroki A, Yoshida J. Electrical resistance change of unidirectional CFRP due to applied load. JSME Int J, A 2004;47(3):357–64.
[18] Todoroki A, Yoshida J. Apparent negative piezoresistivity of single-ply CFRP due to poor electrical contact of four probe method. Key Eng Mater 2005;297–300:610–5.
[19] Wang S, Chang DDL. Negative piezoresistivity in continuous carbon fibre epoxy–matrix composites. J Mater Sci 2007;42(13):4987–95.